Extended capability of the integrated transport analysis suite, TASK3D-a, for LHD experiment

Extended Capability of the Integrated Transport Analysis Suite, TASK3D-a, for LHD Experiment

M. Yokoyama[1,2], R. Seki[1], C. Suzuki[1], M. Sato[1], M. Emoto[1], S. Murakami[3], M. Osakabe[1,2], T. Ii. Tsujimura[1], Y. Yoshimura[1], T. Ido[1], K. Ogawa[1,2], S. Satake[1,2], Y. Suzuki[1,2], T. Goto[1], K. Ida[1,2], N. Pablant[4], D. Gates[4], F. Warmer[5], P. Vincenzi[6], Numerical Simulation Reactor Research Project[1] and LHD Experiment Group[1]

[1]National Institute for Fusion Science, National Institutes of Natural Sciences, Toki 509-5292, Japan
[2]SOKENDAI, Toki 509-5292, Japan
[3]Department of Nuclear Engineering, Kyoto University, Kyoto 615-8540, Japan
[4]Princeton Plasma Physics Laboratory, Princeton, New Jersey 08543, USA
[5]Max-Planck Institute for Plasma Physics, Greifswald D-17491, Germany
[6]Consorzio RFX, Corso Stati Uniti 4, 35127 Padova, Italy

E-mail contact of main author: yokoyama@LHD.nifs.ac.jp

Abstract. The integrated transport analysis suite, TASK3D-a (Analysis), has been developed to be capable for routine whole-discharge analyses of plasmas confined in three-dimensional (3D) magnetic configuration such as the LHD. The routine dynamic energy balance analysis for NBI-heated plasmas was made possible in the first version released in September 2012. The suite has been further extended through implementing additional modules for neoclassical transport and ECH deposition for 3D configurations. The module has also been added for creating the systematic data for the International Stellarator-Heliotron Confinement and Profile Database (ISH-DB). Improvement of NBI modules for multiple-ion species plasmas and a loose-coupling with a large-simulation code are also highlights of recent development.

1. Introduction

Several integrated analysis suites have been developed and applied extensively for tokamaks. It has also been aimed in the framework of IMEG (Integrated Modelling Expert Group) to establish unified integrated analysis suite, so called IMAS (Integrated Modelling and Analysis Suite), for ITER operation [1].

On the other hand, the integrated transport analysis suites had not been such actively developed and applied in Stellarator-Heliotron (S-H) research. A few examples of such integrated transport analysis suites employed in S-H research are PROCTR (mainly based on analytic formulae for physics descriptions) [2], ASTRA (also for tokamaks, solving user-defined set of equations) [3], and NTSS (mainly predictive for Wendelstein 7-X [4] operations so far) [5].

We have launched programmatic efforts for TASK3D-a ("a" stands for analysis) development by incorporating modules for 3D configurations (such as equilibrium and NBI deposition calculations) in the TASK suite [6] for tokamaks. We also have put emphasis on enhancing the interlinkage between TASK3D-a and LHD experiment data [7] which have been lacking in above mentioned integrated codes for S-H research, so that routine-based whole-discharge

and dynamic transport analyses [8] are possible. This is the significant feature of TASK3D-a to facilitate the dynamic transport analyses and increase the physics understandings of LHD plasmas. These TASK3D-a capabilities have been already utilized in several papers [eg., 9,10,11].

2. Significance and Capability Extension of TASK3D-a

Figure 1 shows the TASK3D-a calculation flow. The "a01" stands for the part of its first version (Sep. 2012), and "a02" for the recently-extended parts. The "a01" consists of four parts: LHD data interface, 3D equilibrium, heating (only NBI), and energy balance analysis. The LHD data interface part automatically transfers experiment data registered on the LHD Analysed Data Server. Then the coordinate mapping from the real coordinates to effective minor radius (r_{eff}) is performed by utilizing measured electron temperature (T_e) data to search and pick up the "best-fit" equilibrium in a pre-calculated VMEC [12] database (so called TSMAP [13]). Here, the "best-fit" is considered to satisfy the in-out symmetry (with respect to the magnetic axis position identified by the peak of T_e). This provides the density and temperature profiles for all the timings of T_e measurement as a function of minor radius, which are compatible as inputs to TASK3D-a. Appropriate 3D equilibrium is identified based on this coordinate mapping (that is, the equilibrium identified above), and it is transferred to NBI deposition calculation, in which slowing down process of beam particles is also taken into account. The evaluated NBI heating power is given to the energy balance analysis part, where the experimental energy balance is estimated in a dynamic manner (evolution of density and temperature profiles are taken into account).

The significance of TASK3D-a is to make dynamic transport analyses of LHD easily available. This is explained by referring Fig. 2 which comparatively illustrates the ways of energy transport analysis. Conventionally (left side of Fig. 2), diagnostic data is registered onto the experiment database, and the data for a single (or a few) time slice(s) are extracted, and then mapped onto the effective minor radius (based on equilibrium calculation), and then the equilibrium and profile information are passed to the heating and energy balance analysis. Then, users can obtain 1D (that is, depending on minor radius (r) only) transport analysis results such as ion and electron heat diffusivities, $\chi_i(r)$ and $\chi_e(r)$. Moreover, typically several people involved in this process, and took a time to obtain the final result. On the contrary (right side of Fig. 2), TASK3D-a has made "data integrated" transport analysis possible by means of its automated calculations with full use of experiment database. It extracts all the time-slice information, and these are mapped onto the effective minor radius based on TSMAP, and then heating and energy balance analyses are performed to provide 2D (depending on time (t) in addition to radius) transport analysis results, that are, $\chi_i(r,t)$ and $\chi_e(r,t)$. It should be noted that increased physics understandings based on dynamic transport analyses described such as in Ref. [9,10] are based on the TASK3D-a development and application.
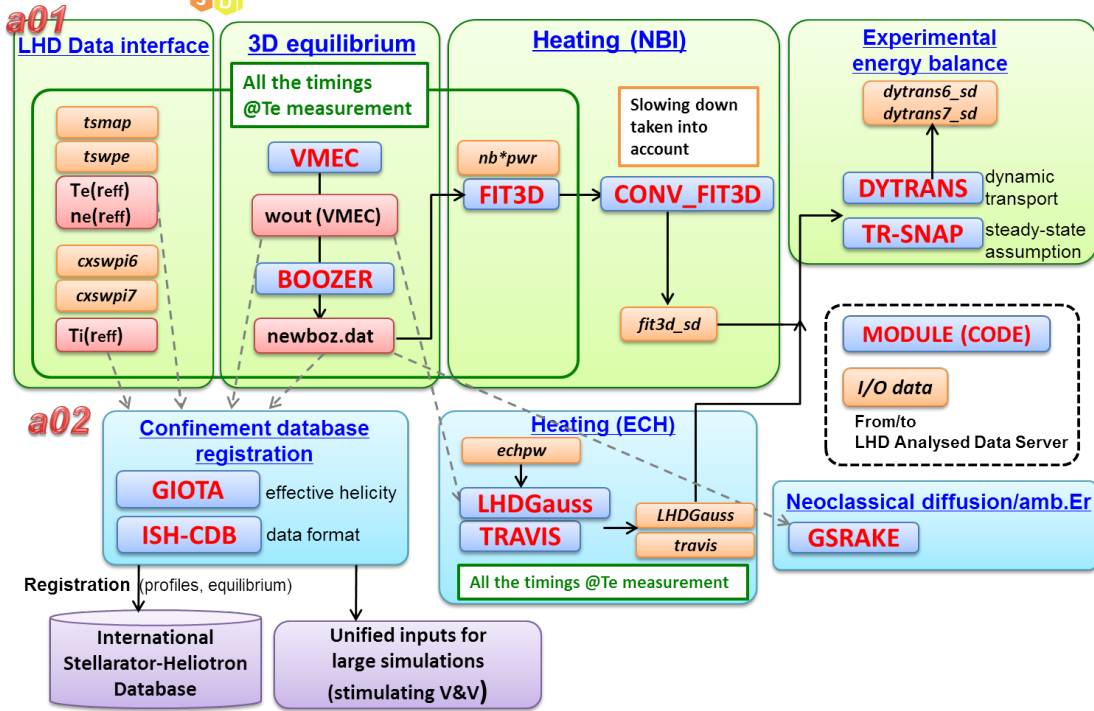
Fig.1: Calculation flow of TASK3D-a ("a01" released in Sep. 2012, and "a02" for recent extensions). Bold uppercase letters indicate the module (numerical code), and italic ones the I/O data from/to the LHD Analysed Data Server. All the calculations are conducted at all the timings of T_e measurement
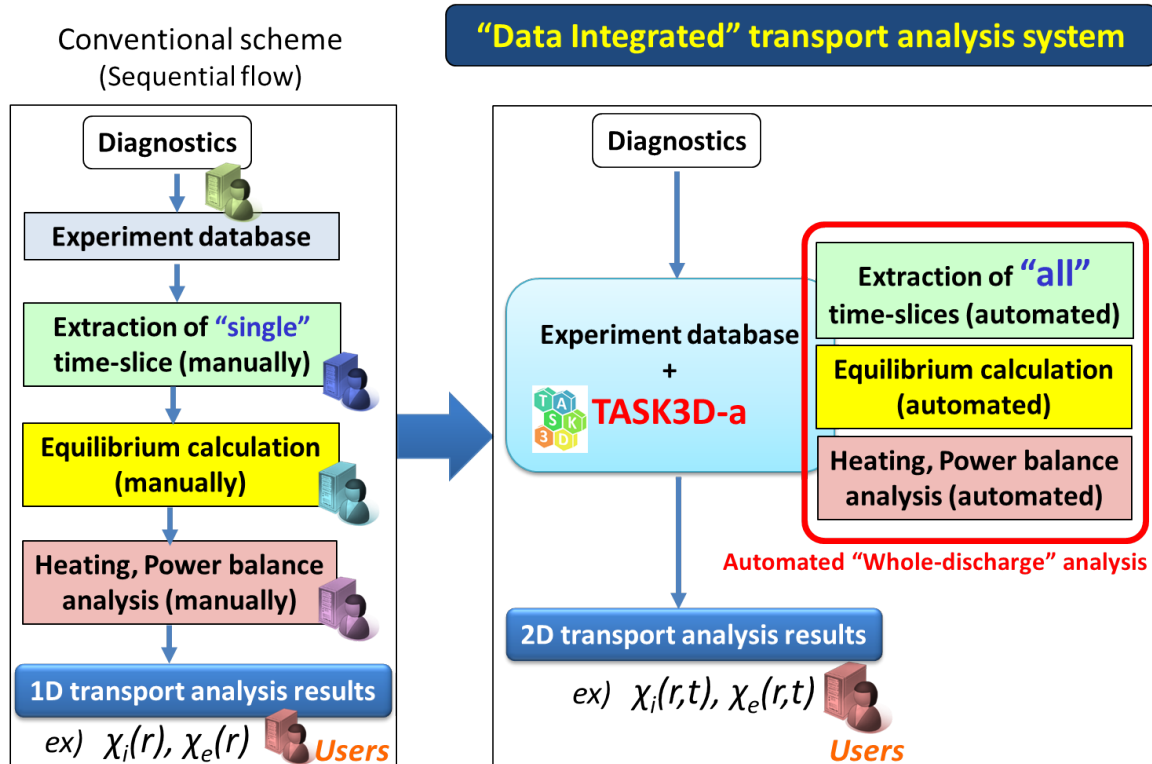

Fig.2: Comparative illustration on approaches of energy transport analysis, (left) conventional (sequential flow with several people involved) approach to provide $\chi_i(r)$ and $\chi_e(r)$, and (right) "data integrated" transport analysis to provide $\chi_i(r,t)$ and $\chi_e(r,t)$, which have been made possible by TASK3D-a development with a linkage to LHD experiment database.

Recently, further extension has been made such as including ECH ray-tracing codes (LHDGauss [14] and TRAVIS [15]), neoclassical transport code, and the module for creating data files to register in the International Stellarator-Heliotron Confinement and Profile Database (module, "ISH-DB", in Fig. 1). Inclusion of ECH ray-tracing code has significantly enhanced capability of systematic energy transport analysis of ECH- (and NBI-) heated LHD plasmas. Neoclassical energy diffusion flux can also be routinely calculated by the implemented GSRAKE code [16], and thus, systematic comparison with experimental energy balance has been available.

Update of NBI module [17] is also the recent highlight which has made capable to apply to plasmas with multiple ions. The neutral beam ionization routine of FIT3D [18] code has been improved to consider the injection of deuterium beams in deuterium plasma with various impurities with the implementation of Suzuki's fit of beam stopping cross sections [19] which is more suitable for a range of NBI injection energy in LHD than Janev's ones [20]. This modification enables the analysis of the ionization of deuterium neutral beams in the deuterium experiment in LHD [21], whose results will be reported elsewhere along with the experimental analyses for deuterium plasmas. It is also applicable to target plasmas with multiple ions such as hydrogen, helium and carbon. Carbon ion (C^{6+}) density profile is measured by charge exchange spectroscopy (CXS) [22], and the ratio between hydrogen ion (H^+) and helium ion (He^{2+}) is obtained by spectroscopic measurement at peripheral region [23]. H^+ and He^{2+} profiles are deduced from the charge neutrality condition with assuming the measured H^+/He^{2+} ratio at the periphery is radially constant. In this way, density profiles of multiple ions are routinely prepared in LHD experiment database for NBI deposition calculations. It has recently been capable through CXS measurement to estimate radial profiles of H^+ and He^{2+} separately [24], and such progress will be reflected on this preparation flow of radial density profiles of multiple ion species. This "multiple-ions" version of TASK3D-a has been released as TASK3D-a03.

Presently, TASK3D-a calculations are performed on 3 workstations with 12 processor cores (24 threads/workstation). Maximum parallel calculations are only 5 at this moment for one discharge analysis because of parallel calculations of several discharges. This number, 5, comes from the number of NBIs. The default timing selection is based on Te profile measurement (30 Hz) so that the whole discharge analysis for a typical 3-seconds discharge takes about 30 hours. Of course, this can be much reduced with increasing parallel calculations and computer resources.

3. Application of TASK3D-a to a LHD discharge (examples of analyses results)

Here in this section, typical analysis results obtained by TASK3D-a run are exemplified by taking one LHD discharge. In this example LHD discharge (shot number: 130345), plasma was started-up with ECH at 3.2 s, and two perpendicular NBIs (NBI #4 and #5) were injected alternately from 3.3 s with modulation for Ti measurement. Three tangential NBIs (NBI #1, #2 and #3) were injected from ~4.5 s along with ECH (4 gyrotrons, 2 of which are 77 GHz and the others are 154 GHz). The heating scenario for this discharge is graphically shown in Fig. 3(a) (left for ECH, and right for NBI injection pattern). Single TASK3D-a run (the job submission, *go_a02, 130345, time=[3.94,4.04,4.14,,,,,6.14,6.24,6.34]* (specifying timings with Ti profile being available, also for reducing the total computation time) provides the time

dependent heating power (NBI slowing down is taken into account by "CONV_FIT3D" module) as shown in Fig. 3(b) (left for ECH, and right for NBI [deposition to ion and electron, respectively]. Arrays in the vertical direction correspond to the radial profiles.) In this example, ECH heating power is evaluated by LHDGauss (Actually, LHDGauss calculations are performed automatically when all the necessary data are ready after conducting discharges, and those calculation results are registered onto the LHD Analyzed Data Server [25]. TASK3D-a reads this registered data in the "Heating (ECH)" part.)

The main physics theme of this example shot is the investigation of the transition of radial electric field (Er). For this purpose, HIBP (Heavy Ion Beam Probe) [26] measurement for electric potential and then deducing Er profiles were performed as shown in Fig. 4(a). The time-averaging (0.3 ~ 0.4 s) is done to obtain reasonable signal to noise ratio. During the superposition of ECH (4.5 ~ 6.0 s), deduced Er becomes positive (so-called electron root) in a certain radial range, in contrast to close to zero or negative values (so-called ion root) in the phase without ECH injection. Corresponding neoclassical transport analyses are also automatically made by GSRAKE module in TASK3D-a run, to provide neoclassical ambipolar Er values as shown in Fig. 4(b). It is found that multiple (3) roots can exist for two timings in the phase of ECH injection, in accordance to the appearance of positive Er in Fig. 4(a). Although the radial range and the Er values themselves are different each other, it is recognized that neoclassical ambipolar Er can provide reasonable guess for the transition property of Er, as previously recognized in several papers such as Ref. [27,28].

The time-dependent heating power shown in Fig. 3(b) is transferred to transport analysis part, TR-SNAP (steady-state assumption) and DYTRANS (dynamic transport), to obtain, for example, experimental ion and electron heat diffusivity profiles for multiple timings, $\chi_i(r,t)$ and $\chi_e(r,t)$, by a single job of TASK3D-a. In the meantime, neoclassical ion and electron heat diffusivities are also ready with GSRAKE module. The comparison between dynamic transport analyses and neoclassical calculations on (a) ion and (b) electron heat diffusivities is shown in Fig. 5 for 4 timings designated in Fig. 4. As for ion heat diffusivity $\chi_i(r,t)$, neoclassical values at core region does not change and a large increase is recognized around r_{eff}/a_{99}~0.7, although it stays at small values for positive ambipolar Er, which is the case from HIBP measurement (cf., Fig. 4(a)). Here, a_{99} is the minor radius in which 99% of the total stored energy is confined. As for electron heat diffusivity $\chi_e(r,t)$, neoclassical values increases almost one order of magnitude for a wide radial region except the region with positive Er. The difference in heat diffusivities between the dynamic transport analyses (eg., experimental power balance) and the neoclassical ones is recognized as the contribution from the turbulent transport. In such a way, comparison between experimental and neoclassical heat diffusivity can be easily made with TASK3D-a run, and then systematic database for contributions from turbulent transport can be created to elucidate those parameter dependences, etc. DYTRANS module can also easily provide data on the flux-gradient relation as shown in Fig. 6, by extracting data for the location of the major radius (R) of 3.879 m (~ r_{eff}/a_{99}~0.4) for (a) ion and (b) electron. The vertical axes correspond to the ion and electron heat flux (including the temporal change of temperature profiles [8]) normalized by the electron density. Response to superposition of NBI#1, #2 and #3 along with ECH at 4.5 s can be recognized by the almost tripled increase of density-normalized heat flux and the increase of temperature gradient (in particular for electron). The slope connecting each point

and the origin of this figure corresponds to the heat diffusivity which is plotted in Fig. 5. It should be noted that, in more transient discharges with wider range of variations in both axes of Fig. 6 (both the heat flux and the temperature gradient), dynamic transport analyses are more crucial to interpret transport nature as reported in Refs. [9,10]. Such crucial data can be easily provided by a single run of TASK3D-a, to facilitate the clarification of transport nature of LHD plasmas.
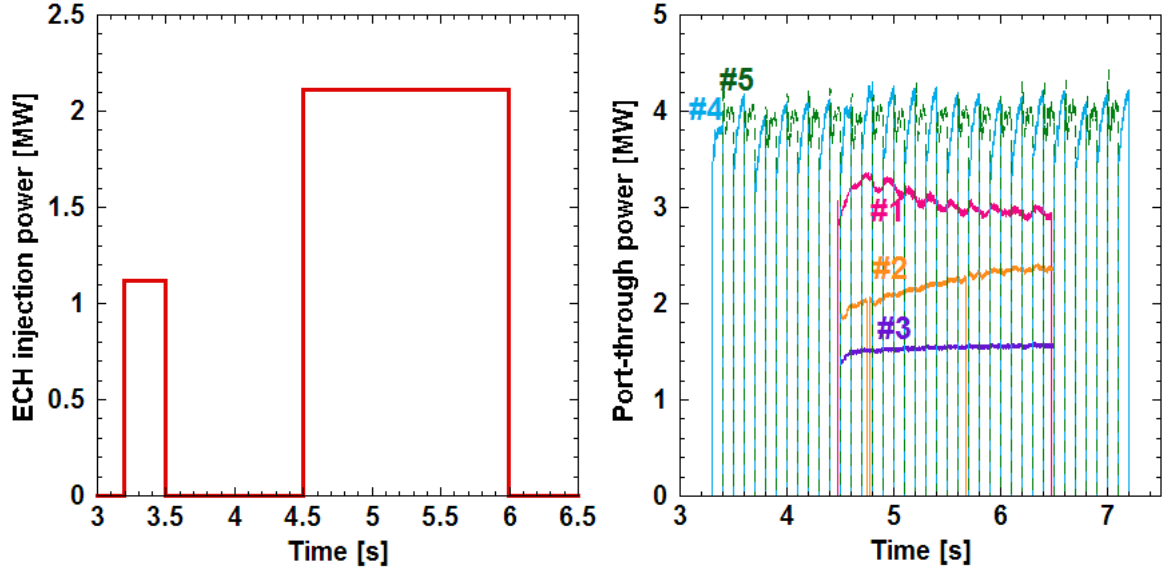

Fig. 3(a) ECH (left) and NBI (right) injection pattern for an example discharge (130345). NBI #4 and #5 are modulated alternately for measuring T_i profile.
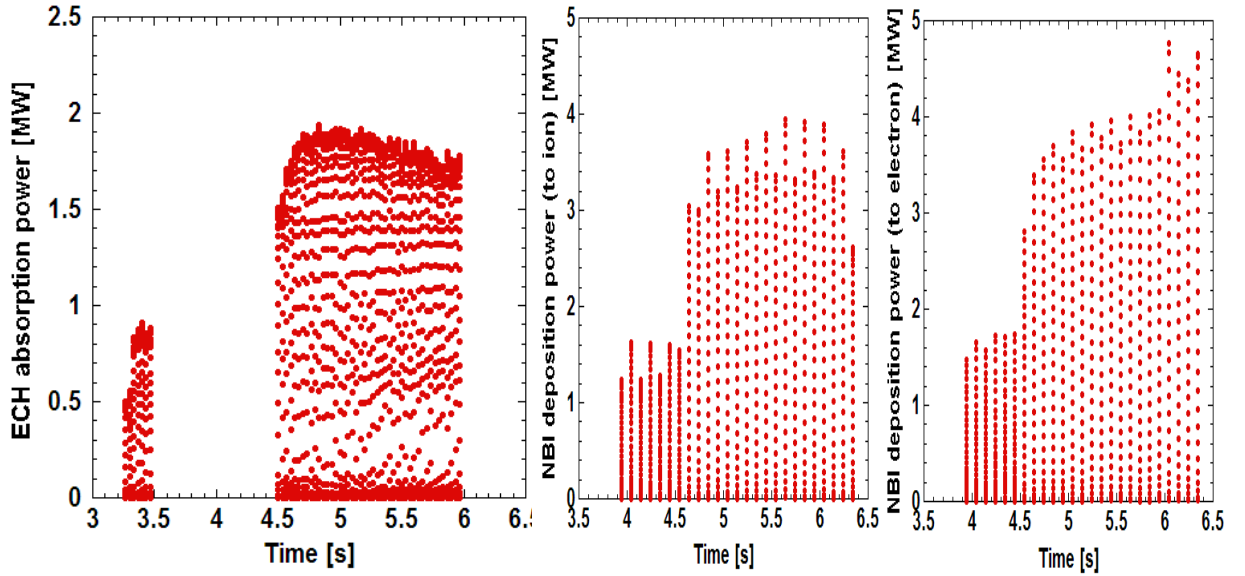
Fig. 3(b) ECH absorption (left) and NBI deposition (to ion and electron) power evaluated by (ECH) LHDGauss and (NBI) FIT3D and CONV_FIT3D (NBI slowing down taken into account) modules based on injection pattern shown in Fig. 3(a).
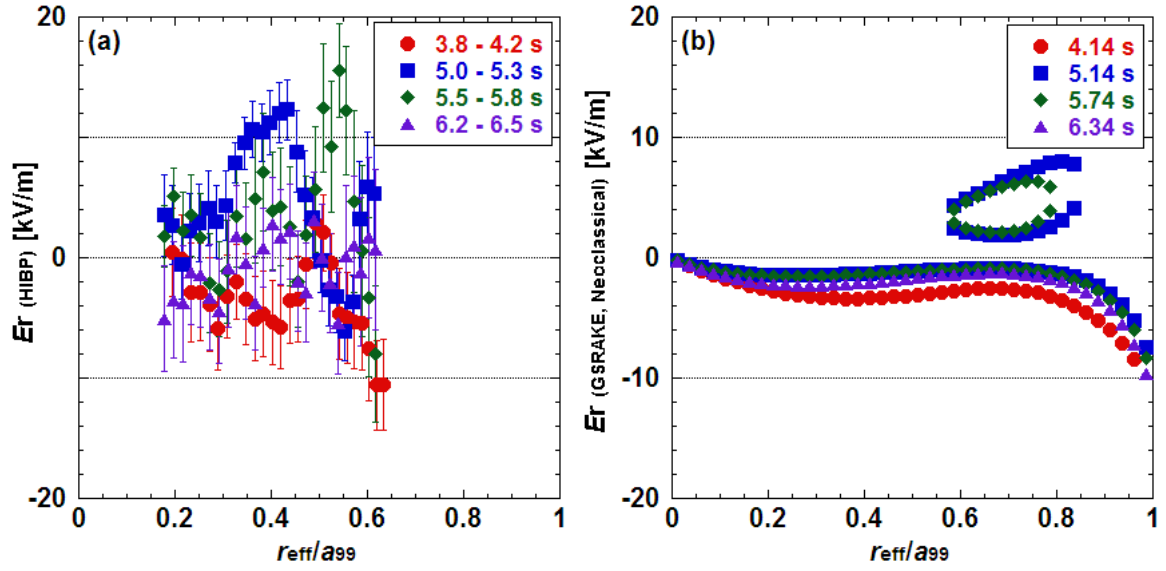
6

Fig. 4 (a) E_r deduced from HIBP measurement for 4 time windows (ECH is injected during 4.5 – 6.0 s), and (b) neoclassical ambipolar E_r for corresponding timings, estimated by GSRAKE module.
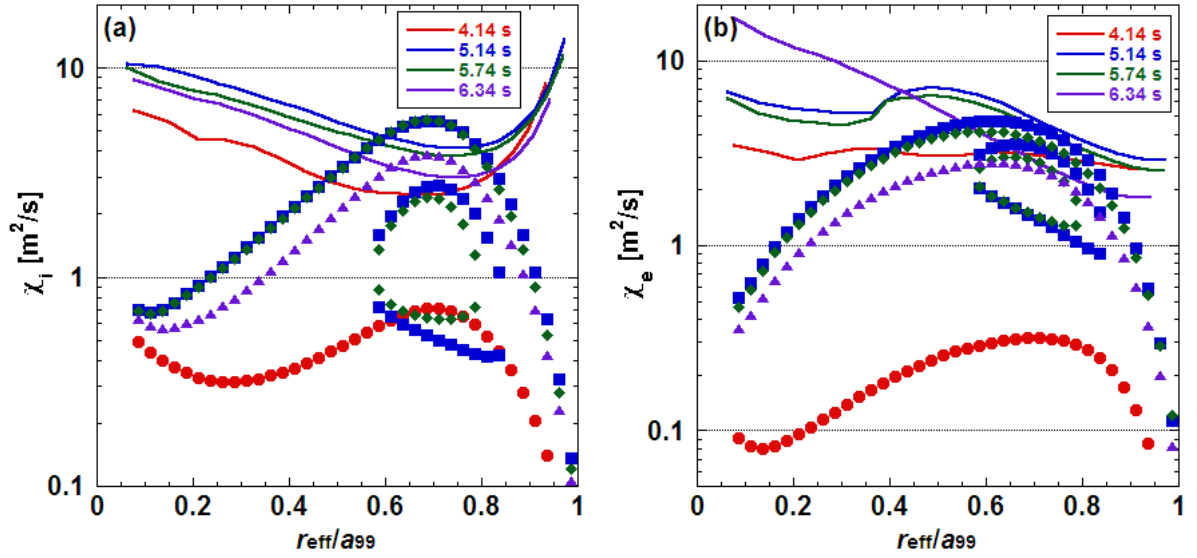

Fig. 5 Comparison between dynamic transport analyses (DYTRANS, solid curves) and neoclassical transport analyses (GSRAKE, dots) on (a) Ion and (b) electron heat diffusivities for 4 timings designated in Fig. 4.
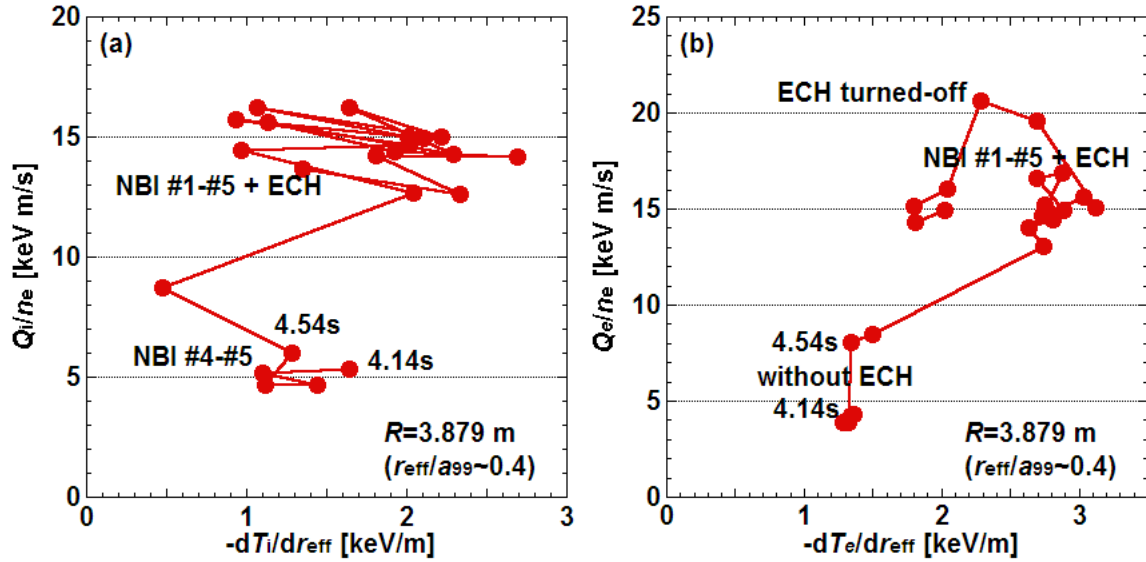
7

Fig. 6 Flux-gradient relation (at R=3.879 m, corresponding to radial location with r_{eff}/a_{99}~0.4) for (a) ion and (b) electron.

4. Another highlighted extension of TASK3D-a; coupling to large-scale simulation codes

All the modules in TASK3D-a had not been computationally intensive, and thus, they can be executed in local servers. However, recently, it has been demanded to implement DKES/PENTA code [29] so that neoclassical particle fluxes of multiple ion species can be evaluated, and the accumulated measurement data for plasmas flows [eg., 30] are systematically compared to the prediction from neoclassical transport simulations. DKES/PENTA code calculates the neoclassical parallel flows, radial particle and energy fluxes, and the radial electric field for a surface given the plasma profiles (density and temperatures, including impurity ions), surface geometry information (from VMEC) and the mono-energetic transport coefficients (from DKES [31]) are provided. It is rather computationally intensive, which practically cannot be applied to whole-discharge analysis in a TASK3D-a environment. However, to facilitate the application of DKES/PENTA to LHD experiment data, a loose coupling to TASK3D-a has been established [32] in a sense that all the necessary files for DKES/PENTA executions are automatically prepared by the TASK3D-a execution. This is also the significance of TASK3D-a, which has demonstrated one of practical ways for broadening physics analyses with large-scale simulations in an integrated environment. The overall calculation flow of DKES/PENTA with a loose coupling with TASK3D-a is schematically summarized in Fig. 7. The VMEC part in Fig. 7 is prepared by TASK3D-a execution along with the necessary files such as execution shells and input files for successive modules. Thus, users just need to copy these necessary files from TASK3D-a server to a large-scale computer, and then to submit the job. This loose-coupling has been facilitating DKES/PENTA applications to LHD discharges [33]. In this way, TASK3D-a will continue to establish loose-coupling to large simulations, to extend the capability of wide-ranging physics analyses of LHD plasmas.
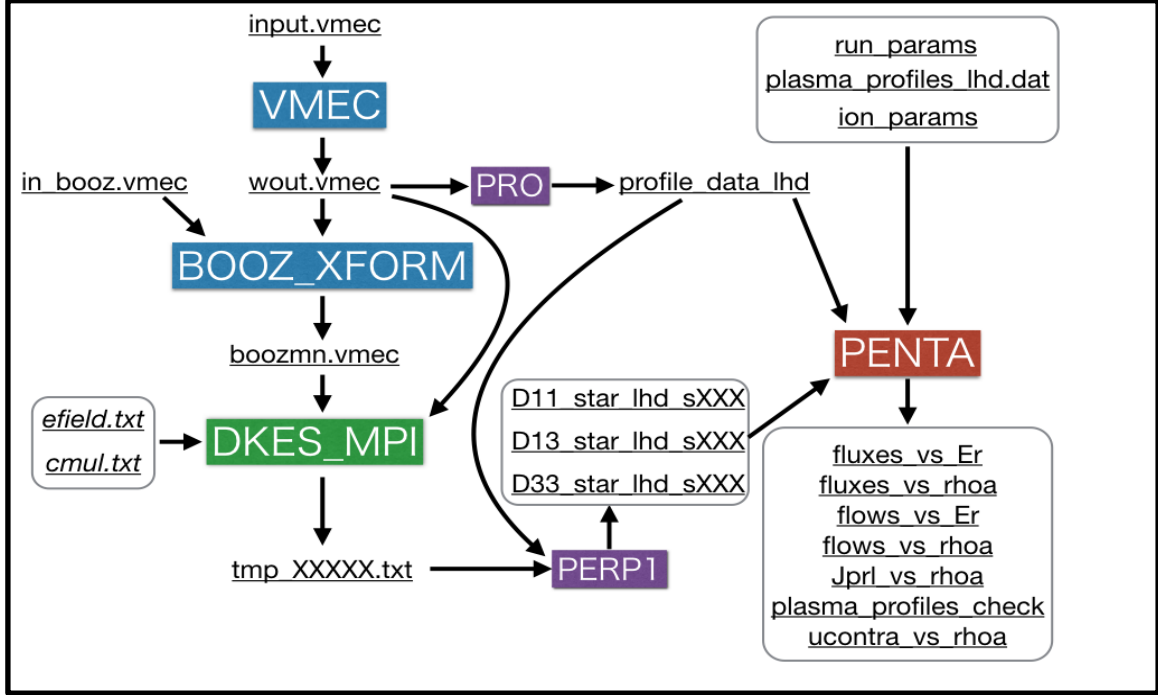
Fig. 7: Overall calculation flow of DKES/PENTA with a loose coupling with TASK3D-a (reproduction from Ref. [32]).

5. Summary and Future Outlook

The integrated transport analysis suite, TASK3D-a (Analysis), has been developed to be capable for routine whole-discharge analyses of plasmas confined in three-dimensional (3D) magnetic configuration such as the LHD. The suite has been further extended through implementing additional modules. However, there are still plenty room for further extension. One of immediate tasks would be to implement particle transport related modules, such as on pellet fuelling, recycling process and impurity transport, so that particle transport issues can be systematically investigated.

Provision of unified equilibrium and temperature/density profiles from TASK3D-a to several simulation codes has facilitated the verification and validation (V&V) activity, as described in Ref. [34]. The International Stellarator-Heliotron Database (Profile Database) is also the appropriate platform to register such unified dataset for facilitating the common use, in addition to the global confinement time database (Confinement Database, having led to the International Stellarator Scaling [35,36]. The data with the compatible format to the Confinement Database has been automatically prepared by TASK3D-a run, and needs to be registered onto the database which has yet been done.

Much further extensions should be pursued towards full-integration by incorporating modules for other physics process. The architecture of TASK3D-a is modularized, and thus transferable to any other Stellarator-Heliotron (even tokamaks) experiments.

9

References

[1] F. Imbeaux, et al., Nucl. Fusion **55** (2015) 123006.

[2] H.C. Howe, "Physics models in the toroidal transport code PROCTR", ORNL/TM-11521 (1990).

[3] G.V. Pereverzev, P.N. Yushmanov, "ASTRA - Automated System for TRansport Analysis", Max-Planck-Institut Fur Plasmaphysik, IPP-Report, IPP 5/98, February (2002).

[4] T. Klinger et al., Plasma Phys. Control. Fusion **59** (2017) 014018.

[5] Y. Turkin et al., Phys. Plasmas **18** (2011) 022505.

[6] A. Fukuyama, http://bpsi.nucleng.kyoto-u.ac.jp/task/.

[7] M. Emoto, et al., "Development and Successful Operation of the Enhanced-Interlink System of Experiment Data and Numerical Simulation in LHD", [FIP/P8-28], paper presented at 25th IAEA Int. Conf. on Fusion Energy St. Petersburg 2014.

[8] H. Lee, et al., Plasma Phys. Control. Fusion **55** (2013) 014011.

[9] K. Ida, et al., Nature Communications, 08 Jan. 2015.

[10] K. Nagaoka, et al., Nucl. Fusion **55** (2015) 113020.

[11] N.A. Pablant, et al., Plasma Phys. Control. Fusion **58** (2016) 045004.

[12] S.P. Hirshman and J.C. Whiston, Phys. Fluids **26** (1983) 3553.

[13] C. Suzuki, et al., Plasma Phys. Control. Fusion **55** (2013) 014016.

[14] T.Ii, Tsujimura, et al., Nucl. Fusion **55** (2015) 123019.

[15] N. Marushchenko, et al., Plasma and Fusion Res. 2 (2007) S1129.

[16] C.D. Beidler and W.D. D'haseleer, Plasma Phys. Control. Fusion **37** (1995) 463.

[17] P. Vincenzi, et al., Plasma Phys. Control. Fusion **58** (2016) 125008.

[18] S. Murakami, et al., Trans. Fusion Technol. **27** (1995) 276.

[19] S. Suzuki, et al., Plasma Phys. Control. Fusion **40** (1998) 2097.

[20] R.K. Janev, et al., Nucl. Fusion **29** (1989) 2125.

[21] Y. Takeiri et al., accepted for publication in Nucl. Fusion (2017), based on "Extension of Operational Regime of LHD towards Deuterium Experiment", [OV/1-1], paper presented at 26th IAEA Int. Conf. on Fusion Energy Kyoto 2016.

[22] M. Yoshinuma, et al., Fusion Sci. Tech. **58** (2010) 375.

[23] M. Goto, et al., Phys. Plasmas **10** (2003) 1402.

[24] K. Ida, et al., Rev. Sci. Instrum. **86** (2015) 123514.

[25] M. Emoto et al., Fusion Eng. Design **81** (2006) 2019.

[26] T. Ido et al., Plasma Fusion Res., **3** (2008) 031.

[27] K. Ida et al., Nucl. Fusion **45** (2005) 391.

[28] M. Yokoyama et al., Fusion Sci. Technol. **58** (2010) 269.

[29] D.A. Spong, et al., Phys. Plasmas **12** (2005) 056114.

[30] K. Ida, et al., Nucl. Fusion **50** (2010) 064007.

[31] S.P. Hirshman, et al., Phys. Fluids **29** (1986) 2951.

[32] M. Sato, et al., NIFS memo 76 (Aug. 31, 2016).

[33] M. Nunami et al., "Anomalous and Neoclassical Transport of Hydrogen Isotope and Impurity Ions in LHD Plasmas", Preprint: 2016 IAEA Fusion Energy Conference, Kyoto [TH/P2-3].

[34] M. Sato, et al., J. Plasma Fusion Res. **93** (2016) 67 (in Japanese).

[35] U. Stroth et al., Nucl. Fusion **36** (1996) 1063.

[36] H. Yamada et al., Nucl. Fusion **45** (2005) 1684.